plasma

MDPI

Article

Polymerization of Sodium 4-Styrenesulfonate Inside Filter Paper via Dielectric Barrier Discharge Plasma

Samira Amiri Khoshkar Vandani, Lian Farhadian, Alex Pennycuick and Hai-Feng Ji *

Department of Chemistry, Drexel University, Philadelphia, PA 19104, USA; sa3948@drexel.edu (S.A.K.V.); lf624@drexel.edu (L.F.); ap3695@dragons.drexel.edu (A.P.)
* Correspondence: hj56@drexel.edu

Abstract: This work explores the polymerization of sodium 4-styrenesulfonate (NaSS) inside filter paper using dielectric barrier discharge (DBD) plasma and its application in the environmental field. The plasma-based technique, performed under mild conditions, solves common problems associated with conventional polymerization inside porous materials. The polymerization process was monitored using Fourier-transform infrared (FTIR) spectroscopy, which confirmed the consumption of double bonds, particularly in NaSS samples containing the optimal concentration of crosslinker divinyl benzene (DVB) (0.25% wt). Our work demonstrates the effectiveness and promise of DBD plasma as a substitute polymerization approach, especially for those in porous materials.

Keywords: DBD plasma; non-thermal plasma; sodium 4-styrenesulfonate; poly (styrene sulfonate)

Citation: Amiri Khoshkar Vandani, S.; Farhadian, L.; Pennycuick, A.; Ji, H.-F. Polymerization of Sodium 4-Styrenesulfonate Inside Filter Paper via Dielectric Barrier Discharge Plasma. *Plasma* **2024**, *7*, 867–876. https://doi.org/10.3390/plasma7040047

Academic Editor: Bruno Caillier

Received: 10 October 2024
Revised: 3 November 2024
Accepted: 7 November 2024
Published: 11 November 2024

1. Introduction

Dielectric barrier discharge (DBD) plasma is a type of electrical discharge that occurs between two electrodes separated by an insulating dielectric barrier. This methodology is particularly effective in producing non-thermal plasmas, which can be generated under atmospheric pressure [1]. The dielectric barrier is a solid material that can prevent the formation of a continuous arc discharge and promote the creation of micro discharges [2]. Unlike thermal plasmas, DBD plasma works at low temperatures, making it a suitable device for applications involving heat-sensitive materials [3]. DBD plasma is cost-effective compared to other types of plasma because it does not require expensive vacuum systems since it can be generated under ambient conditions [4].

The high-energy electrons in DBD plasma can initiate various chemical reactions while keeping the bulk gas at low temperatures, making it an efficient tool for numerous applications. DBD plasma finds use across various fields, including industry, environmental science, and biotechnology. It is widely used for ozone generation in water treatment, air purification, and pollution control, particularly for removing volatile organic compounds (VOCs) [5]. Industrial uses include food packaging, medical equipment sterilization, and the synthesis of chemicals such as nanoparticles. For example, DBD plasma has been used to modify mesoporous silica nanoparticles (MSNs) to create a dual pH and temperature-responsive drug delivery system [6]. Additionally, it has been employed in energy-efficient polymerization processes, such as those involving acrylic acid [7], polyaniline [8], and solid D-ribose [9], without the need for external initiators. Furthermore, DBD plasma has been used to synthesize conductive paper hybrids by polymerizing bithiophene monomer directly into paper [10]. In environmental applications, DBD plasma plays a crucial role in wastewater treatment, including the degradation of perfluorooctanoic acid, a known groundwater pollutant [11]. In biological systems, it has been used to enhance cell transfection [12] and promote wound healing [13]. Recently, DBD plasma has been shown to be a time-efficient method for synthesizing molecularly imprinted polymers (MIPs), which demonstrates enhanced selectivity compared to traditional methods [14]. Additionally,

DBD plasma has been employed in decomposing sugars, polymerizing conductive materials, and modifying polymers for rapid and selective lithium-ion separation in the battery industry [15,16]. DBD plasma applications also extend to engineering fields, including flow control and ice mitigation [17–20]. Despite its wide range of applications [21–23], it is not commonly used in the polymerization process.

In our previous work, we demonstrated that DBD plasma could initiate the radical polymerization of monomers within porous materials, such as cellulose paper, creating paper-based electronics [10] and water-absorbing papers [7]. In this study, we extend our exploration of DBD plasma for its environmental applications in porous materials.

Poly (styrene sulfonate) (PSS) is a synthetic polymer [24] produced by either the sulfonation of polystyrene or the polymerization of sodium 4-styrenesulfonate (NaSS) [25,26]. Its structure consists of a polystyrene backbone with sulfonate groups attached to the benzene rings, giving PSS its anionic polyelectrolyte properties [27–30]. PSS has numerous industrial and biomedical applications [31], including its use in ion-exchange resins, dispersants, stabilizers, and as a sizing and finishing agent in the paper and textile industry, etc. [32–34]. Its ability to remove ions from solutions makes it valuable in water softening and purification processes.

We hypothesized that doping porous materials with PSS could create materials capable of removing toxic chemicals for environmental applications. Traditional methods for synthesizing PSS on porous materials, however, pose challenges. The sulfonation of polystyrene requires strong acids (e.g., sulfur trioxide or chlorosulfonic acid), which can degrade certain materials [35,36]. Alternatively, polymerizing NaSS using ultraviolet (UV) radiation [37] or heat [38] can also be problematic, as heat-initiated polymerization can damage some materials [39], and UV polymerization typically achieves only partial polymerization in deeper layers due to limited photon penetration [40,41].

In contrast, DBD plasma can generate radical initiators in situ and penetrate porous materials, initiating polymerization internally under mild conditions [42]. This makes DBD plasma a safer alternative for synthesizing PSS within porous materials. In this study, we tested the use of DBD plasma to induce the polymerization of sodium 4-styrenesulfonate (NaSS) with N,N′-methylenebisacrylamide (MBAA) to form a stable polymer network inside porous filter paper and assessed its effectiveness in removing waste chemicals from water.

Methylene blue was used in these experiments as a test toxic chemical. Methylthionine chloride, commonly known as methylene blue (chemical formula $C_{16}H_{18}ClN_3S$), is widely used both as a dye and a therapeutic agent [43,44]. However, methylene blue is also considered an environmental pollutant, as its persistence in aquatic environments can lead to toxicity in marine organisms and disrupt ecosystems [45–52]. PSS is recognized as an effective material for methylene blue adsorption due to its anionic sulfonate groups ($–SO_3^-$), which form strong ionic interactions with the cationic dye molecules [45].

2. Materials and Methods

2.1. Materials

N,N′-methylenebisacrylamide (MBAA) was purchased from TCI America (Portland, OR, USA). Distilled water (DI), 4-Stryenesulfonate (NaSS) (Aldrich Chemical, Milwaukee, WI, USA), and divinyl benzene (DVB) was purchased from Electron Microscopy Science (Hatfield, PA, USA).

2.2. DBD Plasma Generation

The DBD plasma was generated using a microsecond-pulsed power supply (FID Technology, Burbach, Germany) and an electrode–dielectric barrier discharge setup, as described previously [7]. In summary, the DBD electrode operates by producing a plasma stream between a high-voltage copper plate (25 mm thick) and a grounded electrode (Figure 1). A 1 mm thick quartz dielectric plate serves as an insulating barrier over the copper plate. The plasma discharge gap between the bottom of the quartz plate and the

sample surface was 5 mm. Plasma was generated using a variable voltage and frequency power supply, which applied a pulsed alternating polarity voltage of 20 kV (peak-to-peak) with a 10 ns pulse width and a rise time of 5 V/ns. For all experiments, a peak voltage of 11.2 kV and a repetition frequency of 690 Hz were used. The input energy was calculated to be approximately 10 mJ per pulse. The plasma treatment area corresponded to the dimensions of the copper plate, measuring 38 mm × 64 mm.

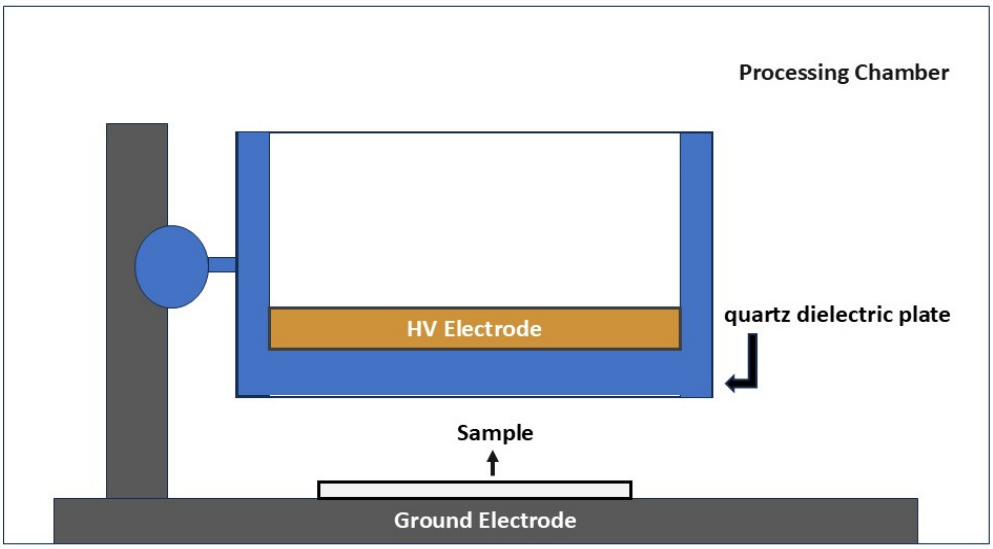

Figure 1. Scheme of DBD Plasma device.

2.3. DBD Plasma Polymerization of NaSS Monomer

A total of 2 g of NaSS monomer is dissolved in 10 mL of DI water, and 3 other samples were made following the same setup, adding varying amounts of MBAA based on weight relative to the NaSS (Sample 1: 0.1%, Sample 2: 0.25%, and Sample 3: 0.5%). A total of 5 microliter aliquots of the samples were then dropped onto silicon wafers, which were placed on glass slides for transporting. The slides with the wafers and the aliquots were brought to the plasma well, where they were exposed to the plasma for 3 min intervals—9 and 15 min in total.

The consistent distance of 5 mm between the quartz plate and the sample surface, combined with the defined plasma area (38 mm × 64 mm) from the copper plate, supports even plasma exposure across the wafer. The carefully controlled parameters, including peak voltage, pulse width, and frequency, contribute to a uniform discharge. However, some factors, such as slight variations in sample positioning on the wafers, potential drying of the NaSS solution, and even plasma distribution, can affect the uniformity. Adding DI water to prevent drying could help mitigate these inconsistencies. While these factors generally support an even polymerization process, slight variations could still occur, especially near the edges of the wafer.

The slides would be removed between intervals to check for signs of polymerization (color change to yellow) and to see if the aliquot was drying out. If there were signs of the aliquot drying out, the sample would add 5 microliters of DI water to keep the solution intact. This was not performed between all intervals to prevent samples from spilling from the wafers or for excess liquid to stick to the bottom of the plasma well. After the plasma treatments (3 or 5 intervals), the samples were taken out and left on the lab bench to air dry overnight. This can be seen in Figure 2.

Figure 2. Deposits of polymerized sodium styrene sulfonate on silicon wafers.

2.4. IR and FT-IR Characterization and Analysis

A PerkinElmer Spectrum One FTIR Spectrometer (Waltham, MA, USA) was employed to capture samples' Fourier-transform infrared (FTIR) spectra before and after DBD plasma treatment. FTIR measurements were conducted using attenuated total reflection (ATR), covering the spectral range from 650 cm^{-1} to 3650 cm^{-1} with a resolution of 4 cm^{-1}. Before and after polymerization by plasma, the samples were scanned by the FTIR spectrometer, having the silicon wafers placed sample side down onto the diamond of the spectrometer and then scanned.

2.5. Hydrophilicity Test Analysis

It is crucial to assess the polymers' compatibility with water-based solutions, their potential for biomedical applications, and how they will function in aqueous reaction environments [51]. The hydrophilicity test is commonly employed to evaluate polymers' capacity to attract and hold water. There are multiple methods to examine how a polymer interacts with water, encompassing water absorption testing, surface energy calculation, and the predominant one, contact angle measurement. The final method measures the contact angle between the water droplet and the polymer surface by placing the droplet on the polymer surface. This contact angle serves as a pivotal indicator of the polymer's hydrophilicity. If the water droplet beads up on the polymer surface, this high contact angle demonstrates low hydrophilicity, while a low contact angle, where the water spreads out on the polymer surface, indicates high hydrophilicity. Since PSS is considered a hydrophilic polymer, the samples were also tested for hydrophilicity by adding 3 microliter drops to dried samples and observing the resulting contact angle of the liquid.

2.6. Methylene Blue Removal Analysis

This analysis used PSS with two crosslinkers to study their effect on removing methylene blue (MB) from water. For this experiment, 0.001 g of MB was dissolved in 200 mL of DI water, and its UV-Vis spectrum was recorded. Three samples of PSS containing varying amounts of MBAA, as described in Section 2.3, were prepared alongside samples with the same ratios using DVB as the crosslinker. Filter papers were soaked in each solution and exposed to DBD plasma for 20 min to form polymers on the filter paper. The MB solution was then filtered through all six polymer-coated filter papers and a regular filter paper for comparison. The UV-Vis spectra of all filtrates were collected for comparison.

The MB removal efficiency of the prepared papers after filtration was calculated by using Equation (1) as follows:

$$\text{Efficiency} = (C_i - C_f/C_i) \times 100 \quad (1)$$

C_i and C_f are the initial and final concentrations of MB in solution, measured at 665 nm [53].

3. Results

3.1. Characterization of PSS Using Infrared Spectroscopy

We first demonstrated the use of DBD plasma to induce the polymerization of sodium 4-styrenesulfonate (NaSS). The resulting FTIR scans are shown in Figure 3.

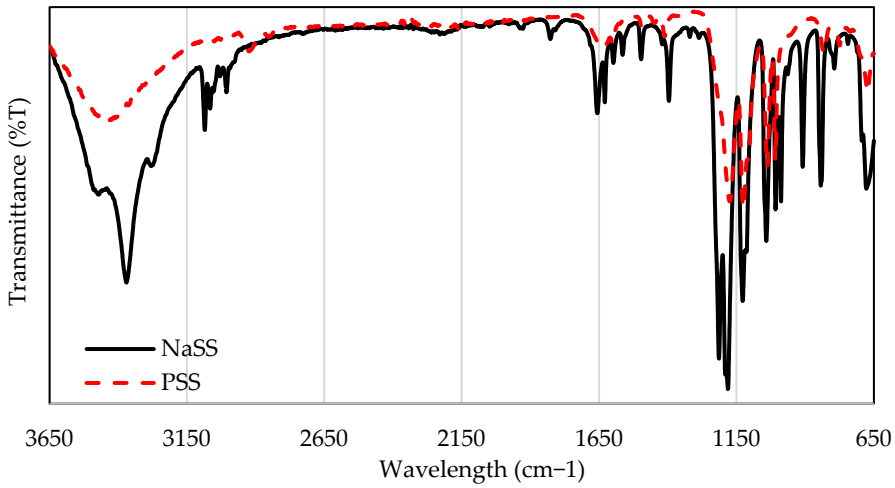

Figure 3. FTIR spectra of 4-Styrenesulfonate (NaSS) and Poly (styrene sulfonate) (PSS) synthesized from DBD plasma treatment of NaSS.

The primary focus of the IR spectra is the peaks at 985 $\pm$ 5 cm^{-1} and 910 $\pm$ 5 cm^{-1}, which are the peaks associated with the C=C double bonds commonly observed in vinyl compounds. After DBD plasma polymerization, NaSS exhibits the complete disappearance of these peaks, indicating total polymerization of NaSS. This confirms the effectiveness of DBD plasma in inducing NaSS polymerization.

The FTIR spectra of NaSS and PSS closely resemble those reported in the literature, with the major peaks at 985 cm^{-1} and 910 cm^{-1} indicating the completion of the polymerization process. A notable difference observed in our sample, compared to published spectra, is the presence of two distinct peaks in the 3400–3600 cm^{-1} region for NaSS. This suggests the presence of water molecules in two forms: free water and water associated with NaSS via hydrogen bonding. This is not unusual, as varying amounts or interactions of water with the monomer can result in different peaks in this region.

The plasma discharge on the substrate was assumed to be uniform based on prior studies involving DBD plasma. However, due to the NaSS deposition on the wafer surfaces via drop-casting, the resulting film is likely non-uniform. As this study serves as a preliminary investigation for subsequent research on polymerization within porous materials, we did not assess the film's uniformity.

3.2. Formation and Hydrophilic Property of PSS/MBAA and PSS/DVB Polymer Network

PSS is water-soluble, making it prone to being washed out of porous materials when exposed to water. To prevent PSS leakage and enhance the efficiency of PSS-doped porous materials for chemical removal, crosslinkers such as MBAA and DVB were used to co-polymerize with NaSS, forming a networked PSS that is insoluble in any solvent. Figure 4 shows the image of this polymer network. The resulting polymer is insoluble in water, meeting the requirement for doping porous materials to remove toxic chemicals. The polymer was observed to be hydrophilic, as indicated by its very low contact angle (Figure 4). The water contact angle for our sample is roughly 8 $\pm$ 2°.

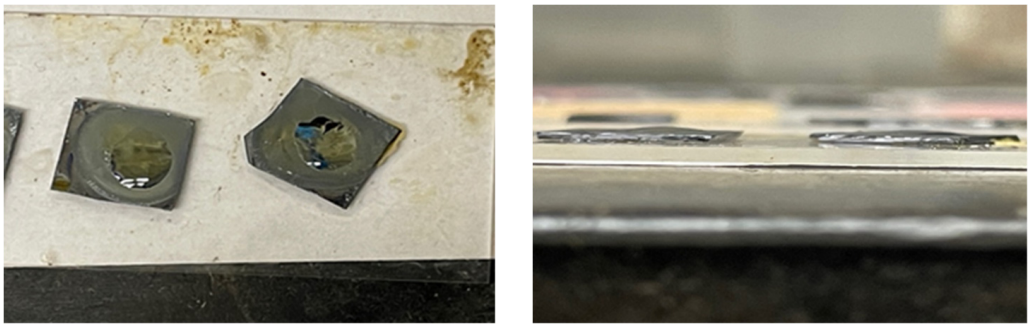

(**a**) (**b**)

Figure 4. Hydrophilicity test of the PSS/DVB and PSS/MBAA polymer network. (**a**) left slide is for PSS/DVB and the right slide is PSS/MBAA. (**b**) left slide is for PSS/DVB and the right slide is PSS/MBAA.

3.3. Methylene Blue Water Pollutant Removal

For proof-of-concept, filter paper doped with PSS was tested for its methylene blue (MB) removal efficiency. This test aimed to assess how effectively PSS, crosslinked with varying amounts of MBAA and DVB, could remove MB from the solution. By crosslinking the PSS with these agents inside the filter paper, the polymer becomes more robust and potentially more effective at capturing and filtering out MB due to the enhanced network structure.

The removal efficiency of MB was quantified by comparing different filter papers doped with PSS that had been crosslinked with either MBAA or DVB at various concentrations. As shown in Table 1, the results are the MB removal rates after a single filtration. The study found that PSS crosslinked with 0.5% DVB demonstrated the highest MB removal efficiency, suggesting that this specific concentration of DVB forms an optimal network within the PSS matrix for capturing MB. This highlights the potential of using DVB-crosslinked PSS for applications requiring effective filtration and removal of dye pollutants, such as wastewater treatment.

Table 1. MB removal rates after the first filtration using both PSS/MBAA and PSS/DVB. The uncertainty is determined as ±2%.

Crosslinker	Ratio	MB Removal Rate (%)
MBAA	0.1%	58.22
	0.25%	58.50
	0.5%	63.35
DVB	0.1%	58.54
	0.25%	63.65
	0.5%	68.83

Subsequently, four consecutive filtrations were also performed using blank filter paper and filter paper doped with PSS crosslinked with 0.5% DVB. The results, shown in Table 2, indicate that the PSS/DVB-coated filter paper removed 99.4% of MB after four filtrations, compared to 78.5% removal by the blank filter paper.

Following the initial filtration tests, four consecutive filtrations were performed to further evaluate the long-term MB removal efficiency of the PSS-coated filter paper. Specifically, the one crosslinked with 0.5% DVB, compared to blank filter paper without any PSS coating. This series of tests aimed to determine the sustained filtration capacity and effectiveness of the PSS/DVB system over multiple cycles, simulating practical use scenarios where a filter would need to handle more than one round of filtration.

As presented in Table 2, the results were compelling. After four consecutive filtrations, the PSS-coated filter paper crosslinked with 0.5% DVB achieved a remarkable 99.4% removal

of MB from the solution. This contrasts significantly with the blank filter paper, which only removed 78.5% of MB under the same conditions. The difference in removal efficiency demonstrates the enhanced capability of the PSS/DVB coating in consistently capturing and removing MB molecules over multiple filtration cycles. This performance can be attributed to the stable, crosslinked network of PSS created by DVB, which provides more active sites for MB adsorption and prevents the polymer from dissolving or degrading during filtration. As previously noted, the increased hydrophilicity of the material also likely contributes to its enhanced affinity for MB, facilitating greater contact and interaction between the dye molecules and the filter surface.

Overall, the PSS/DVB-coated filter paper's ability to maintain higher removal efficiency across multiple filtration rounds highlights its potential for practical water purification and dye pollutant removal applications. The durability and effectiveness of this crosslinked system make it a promising candidate for use in large-scale or industrial filtration systems where repeated usage is critical.

Table 2. MB removal rates after four filtration trials using both PSS/DVB and blank filter paper. The uncertainty is determined as roughly ±2%.

Trial	Filter Paper	MB Removal Rate (%)
First	blank	47.80
	PSS/DVB(0.5%)	68.83
Second	blank	67.70
	PSS/DVB(0.5%)	84.41
Third	blank	74.30
	PSS/DVB(0.5%)	95.80
Fourth	blank	78.50
	PSS/DVB(0.5%)	99.40

4. Discussion

The findings of this work show that sodium 4-styrene sulfonate (NaSS) can be polymerized within porous materials, especially filter paper, using dielectric barrier discharge (DBD) plasma. Plasma offers a distinct benefit compared to traditional polymerization techniques like UV or heat-based polymerization, which frequently have drawbacks like inadequate penetration or thermal damage to delicate materials. FTIR measurement shows that the C=C double bonds completely disappear in NaSS, indicating that the DBD plasma successfully triggered polymerization under mild circumstances. This supports the feasibility of DBD plasma for polymerization within porous substrates and is consistent with earlier research using non-thermal plasma for comparable purposes.

The PSS crosslinked with 0.5% divinylbenzene (DVB) with the highest methylene blue elimination efficiency indicates greater stability and longevity of the polymer network. This demonstrates how crosslinked PSS can be used in environmental applications where multiple filtration cycles are necessary, such as wastewater treatment. These findings are consistent with the body of research on the effectiveness of crosslinked polymer systems in environmental cleanup. The applications of DBD plasma-synthesized PSS materials for water treatment would require practical considerations such as material durability, filtration efficiency under variable water conditions, commercialization, and potential fouling. Furthermore, while stable in controlled lab settings, the crosslinked structure may face challenges in natural waters containing competing organic and inorganic materials, which could reduce its adsorption capacity for methylene blue (MB). Thus, optimizing DBD plasma treatment for consistent polymerization quality, testing its stability in various water conditions, and assessing capacity for larger treatment systems are essential to advancing this technique for practical environmental applications. Additionally, the durability of the DBD plasma-modified filter paper in continuous flow systems will also be considered.

Reusability would be advantageous for real-world applications; therefore, regeneration of the filter material when it reaches adsorption capacity is another considerable factor.

The DBD plasma can be generated in various gases, such as N_2, Ar, O_2, air, etc. Although all of them can polymerize monomers to polymers, such as NaSS to PSS, the polymerization process, polymerization efficiency, reaction rate, and properties of polymers vary from different plasmas. Among these, air DBD plasma is the most common plasma due to its lower cost. In our experiments, the DBD plasma was generated in air at ambient conditions. The air–plasma contains reactive oxygen and nitrogen species (ROS and RNS), including ozone (O_3), radicals (•NO and •OH), superoxide anion (O_2^-), and electrons, etc. The radicals are believed to be the species that could initiate the polymerization reaction. Other species, including impurities in air, do not significantly affect the polymerization process and the properties of the polymers.

Subsequent investigations may concentrate on the feasibility of this methodology for commercial implementations and examine alternative monomers and crosslinkers for constructing customized polymer networks. Additionally, researching the long-term stability of these systems in real-world climatic circumstances would provide greater insight into their practical usage. Another area worth investigating is combining DBD plasma polymerization with other environmentally friendly technologies to create integrated systems for resource recovery or pollution management.

5. Conclusions

The FTIR data demonstrates that DBD plasma treatment effectively induces polymerization of sodium 4-styrene sulfonate (NaSS) within porous filter paper and creates a stable PSS matrix crosslinked with N, N-methylene bisacrylamide (MBAA) and divinyl benzene (DVB). The optimized use of DBD plasma under mild conditions enabled thorough polymerization without initiators or excessive thermal energy. Among tested configurations, the PSS crosslinked with 0.5% DVB exhibited the highest methylene blue (MB) removal, up to 99.4%, over four consecutive filtrations. This crosslinked network demonstrates stability and reusability, aligning with sustainable water purification goals. Future directions include investigating this method's scalability, testing additional monomer systems, and developing DBD plasma-modified filter materials with tailored properties for diverse environmental and biomedical applications. These findings highlight the broader potential of non-thermal plasma in creating robust, biocompatible, and efficient polymer-based adsorbents for environmental applications.

Author Contributions: Conceptualization, S.A.K.V. and H.-F.J.; Methodology, A.P. and H.-F.J.; Validation, S.A.K.V.; Formal analysis, S.A.K.V. and H.-F.J.; Investigation, S.A.K.V., L.F. and A.P.; Data curation, L.F. and A.P.; Writing—review & editing, L.F. and H.-F.J. All authors have read and agreed to the published version of the manuscript.

Funding: This research received no external funding.

Data Availability Statement: The original contributions presented in the study are included in the article, further inquiries can be directed to the corresponding author/s.

Conflicts of Interest: The authors declare no conflict of interest.

References

1. Brandenburg, R. Dielectric Barrier Discharges: Progress on Plasma Sources and on the Understanding of Regimes and Single Filaments. *Plasma Sources Sci. Technol.* **2017**, *26*, 053001. [CrossRef]
2. Subedi, D.P.; Joshi, U.M.; Wong, C.S. Dielectric Barrier Discharge (DBD) Plasmas and Their Applications. In *Plasma Science and Technology for Emerging Economies: An AAAPT Experience*; Rawat, R.S., Ed.; Springer: Singapore, 2017; pp. 693–737, ISBN 978-981-10-4217-1.
3. Ollegott, K.; Wirth, P.; Oberste-Beulmann, C.; Awakowicz, P.; Muhler, M. Fundamental Properties and Applications of Dielectric Barrier Discharges in Plasma-Catalytic Processes at Atmospheric Pressure. *Chem. Ing. Tech.* **2020**, *92*, 1542–1558. [CrossRef]
4. He, J.; Wen, X.; Wu, L.; Chen, H.; Hu, J.; Hou, X. Dielectric Barrier Discharge Plasma for Nanomaterials: Fabrication, Modification and Analytical Applications. *TrAC Trends Anal. Chem.* **2022**, *156*, 116715. [CrossRef]

5. Lisi, N.; Pasqual Laverdura, U.; Chierchia, R.; Luisetto, I.; Stendardo, S. A Water Cooled, High Power, Dielectric Barrier Discharge Reactor for CO_2 Plasma Dissociation and Valorization Studies. *Sci. Rep.* **2023**, *13*, 7394. [CrossRef]
6. Porrang, S.; Rahemi, N.; Davaran, S.; Mahdavi, M.; Hassanzadeh, B.; Gholipour, A.M. Direct Surface Modification of Mesoporous Silica Nanoparticles by DBD Plasma as a Green Approach to Prepare Dual-Responsive Drug Delivery System. *J. Taiwan Inst. Chem. Eng.* **2021**, *123*, 47–58. [CrossRef]
7. Mieles, M.; Harper, S.; Ji, H.-F. Bulk Polymerization of Acrylic Acid Using Dielectric-Barrier Discharge Plasma in a Mesoporous Material. *Polymers* **2023**, *15*, 2965. [CrossRef] [PubMed]
8. Chen, K.; Cao, M.; Feng, E.; Sohlberg, K.; Ji, H.-F. Polymerization of Solid-State Aminophenol to Polyaniline Derivative Using a Dielectric Barrier Discharge Plasma. *Plasma* **2020**, *3*, 187–195. [CrossRef]
9. Li, Y.; Atif, R.; Chen, K.; Cheng, J.; Chen, Q.; Qiao, Z.; Fridman, G.; Fridman, A.; Ji, H.-F. Polymerization of D-Ribose in Dielectric Barrier Discharge Plasma. *Plasma* **2018**, *1*, 144–149. [CrossRef]
10. Chen, K.; Cao, M.; Qiao, Z.; He, L.; Wei, Y.; Ji, H.-F. Polymerization of Solid-State 2,2′-Bithiophene Thin Film or Doped in Cellulose Paper Using DBD Plasma and Its Applications in Paper-Based Electronics. *ACS Appl. Polym. Mater.* **2020**, *2*, 1518–1527. [CrossRef]
11. Cheng, J.; Fan, Y.; Pei, X.; Tian, D.; Liu, Z.; Wei, Z.Z.; Ji, H.; Chen, Q. Mechanism and Reactive Species in a Fountain-Strip DBD Plasma for Degrading Perfluorooctanoic Acid (PFOA). *Water* **2022**, *14*, 3384. [CrossRef]
12. Leduc, M.; Guay, D.; Leask, R.L.; Coulombe, S. Cell Permeabilization Using a Non-Thermal Plasma. *New J. Phys.* **2009**, *11*, 115021. [CrossRef]
13. Shekhter, A.B.; Serezhenkov, V.A.; Rudenko, T.G.; Pekshev, A.V.; Vanin, A.F. Beneficial Effect of Gaseous Nitric Oxide on the Healing of Skin Wounds. *Nitric Oxide* **2005**, *12*, 210–219. [CrossRef] [PubMed]
14. Amiri Khoshkar Vandani, S.; Liu, Q.; Lam, Y.; Ji, H.-F. Enhancing Selectivity with Molecularly Imprinted Polymers via Non-Thermal Dielectric Barrier Discharge Plasma. *Polymers* **2024**, *16*, 2380. [CrossRef] [PubMed]
15. Li, Y.; Friedman, G.; Fridman, A.; Ji, H.-F. Decomposition of Sugars under Non-Thermal Dielectric Barrier Discharge Plasma. *Clin. Plasma Med.* **2014**, *2*, 56–63. [CrossRef]
16. Guo, Y.; Ying, Y.; Mao, Y.; Peng, X.; Chen, B. Polystyrene Sulfonate Threaded through a Metal–Organic Framework Membrane for Fast and Selective Lithium-Ion Separation. *Angew. Chem.* **2016**, *128*, 15344–15348. [CrossRef]
17. Rodrigues, F.F.; Shvydyuk, K.O.; Nunes-Pereira, J.; Páscoa, J.C.; Silva, A.P. Plasma Actuators Based on Alumina Ceramics for Active Flow Control Applications. *Ceramics* **2024**, *7*, 192–207. [CrossRef]
18. Kolbakir, C.; Hu, H.; Liu, Y.; Hu, H. An experimental study on different plasma actuator layouts for aircraft icing mitigation. *Aerosp. Sci. Technol.* **2020**, *107*, 106325. [CrossRef]
19. Omidi, J. Advances and opportunities in wind energy harvesting using plasma actuators: A review. *Clean Energy* **2024**, *8*, 197–225. [CrossRef]
20. Shvydyuk, K.O.; Rodrigues, F.F.; Nunes-Pereira, J.; Páscoa, J.C.; Lanceros-Mendez, S.; Silva, A.P. Long-lasting ceramic composites for surface dielectric barrier discharge plasma actuators. *J. Eur. Ceram. Soc.* **2023**, *43*, 6112–6121. [CrossRef]
21. Coolbs, P.; Van Vrekhem, S.; De Geyter, N.; Morent, R. The Use of DBD Plasma Treatment and Polymerization for the Enhancement of Biomedical UHMWPE. *Thin Solid Films* **2014**, *572*, 251–259. [CrossRef]
22. Borra, J.-P.; Valt, A.; Arefi-Khonsari, F.; Tatoulian, M. Atmospheric Pressure Deposition of Thin Functional Coatings: Polymer Surface Patterning by DBD and Post-Discharge Polymerization of Liquid Vinyl Monomer from Surface Radicals. *Plasma Process. Polym.* **2012**, *9*, 1104–1115. [CrossRef]
23. Morent, R.; De Geyter, N.; Van Vlierberghe, S.; Beaurain, A.; Dubruel, P.; Payen, E. Influence of Operating Parameters on Plasma Polymerization of Acrylic Acid in a Mesh-to-Plate Dielectric Barrier Discharge. *Prog. Org. Coat.* **2011**, *70*, 336–341. [CrossRef]
24. Chen, M.; Shafer-Peltier, K.; Randtke, S.J.; Peltier, E. Competitive Association of Cations with Poly(Sodium 4-Styrenesulfonate) (PSS) and Heavy Metal Removal from Water by PSS-Assisted Ultrafiltration. *Chem. Eng. J.* **2018**, *344*, 155–164. [CrossRef]
25. Sepulveda, V.R.; Sierra, L.; López, B.L. Low Dispersity and High Conductivity Poly(4-Styrenesulfonic Acid) Membranes Obtained by Inexpensive Free Radical Polymerization of Sodium 4-Styrenesulfonate. *Membranes* **2018**, *8*, 58. [CrossRef] [PubMed]
26. Kuntz, I. Anionic Polymerization. Kinetics, Mechanisms and Synthesis. *Organometallics* **1982**, *1*, 1106. [CrossRef]
27. Kwon, H.J.; Osada, Y.; Gong, J.P. Polyelectrolyte Gels-Fundamentals and Applications. *Polym. J.* **2006**, *38*, 1211–1219. [CrossRef]
28. Das, S.; Banik, M.; Chen, G.; Sinha, S.; Mukherjee, R. Polyelectrolyte Brushes: Theory, Modelling, Synthesis and Applications. *Soft Matter* **2015**, *11*, 8550–8583. [CrossRef]
29. Yuan, W.; Weng, G.-M.; Lipton, J.; Li, C.M.; Van Tassel, P.R.; Taylor, A.D. Weak Polyelectrolyte-Based Multilayers via Layer-by-Layer Assembly: Approaches, Properties, and Applications. *Adv. Colloid Interface Sci.* **2020**, *282*, 102200. [CrossRef]
30. Thünemann, A.F. Polyelectrolyte–Surfactant Complexes (Synthesis, Structure and Materials Aspects). *Prog. Polym. Sci.* **2002**, *27*, 1473–1572. [CrossRef]
31. Sun, K.; Zhang, S.; Li, P.; Xia, Y.; Zhang, X.; Du, D.; Isikgor, F.H.; Ouyang, J. Review on Application of PEDOTs and PEDOT:PSS in Energy Conversion and Storage Devices. *J. Mater. Sci. Mater. Electron.* **2015**, *26*, 4438–4462. [CrossRef]
32. Chen, S.-L.; Krishnan, L.; Srinivasan, S.; Benziger, J.; Bocarsly, A.B. Ion Exchange Resin/Polystyrene Sulfonate Composite Membranes for PEM Fuel Cells. *J. Membr. Sci.* **2004**, *243*, 327–333. [CrossRef]
33. He, Q.; Wang, X.; Dai, D.; Feng, Y.; Xu, R.; Yan, J.; Wang, P.; Shen, J.; Hu, B. Resource Utilization of Polystyrene Waste by Preparation of High Performance Dispersant for Coal-Water Slurry. *Int. J. Coal Prep. Util.* **2024**, *44*, 920–940. [CrossRef]

34. Tseghai, G.B.; Mengistie, D.A.; Malengier, B.; Fante, K.A.; Van Langenhove, L. PEDOT:PSS-Based Conductive Textiles and Their Applications. *Sensors* **2020**, *20*, 1881. [CrossRef] [PubMed]
35. Coughlin, J.E.; Reisch, A.; Markarian, M.Z.; Schlenoff, J.B. Sulfonation of Polystyrene: Toward the "Ideal" Polyelectrolyte. *J. Polym. Sci. Part Polym. Chem.* **2013**, *51*, 2416–2424. [CrossRef]
36. Dalla Valle, C.; Zecca, M.; Rastrelli, F.; Tubaro, C.; Centomo, P. Effect of the Sulfonation on the Swollen State Morphology of Styrenic Cross-Linked Polymers. *Polymers* **2020**, *12*, 600. [CrossRef]
37. Rymsha, K.V.; Yevchuk, I.Y.; Zhyhailo, M.M.; Demchyna, O.I.; Maksymych, V.M.; Ivashchyshyn, F.O. Hydrogels and Their Composites Based on Sulfo-Containing Acrylates: Preparation, Properties, and Proton Conductivity. *J. Solid State Electrochem.* **2024**, *28*, 555–563. [CrossRef]
38. Liu, H.; Gong, B.; Zhou, Y.; Sun, Z.; Wang, X.; Zhao, S. Preparation of High-Capacity Magnetic Polystyrene Sulfonate Sodium Material Based on SI-ATRP Method and Its Adsorption Property Research for Sulfonamide Antibiotics. *BMC Chem.* **2020**, *14*, 3. [CrossRef]
39. Villermaux, J.; Blavier, L. Free Radical Polymerization Engineering—I: A New Method for Modeling Free Radical Homogeneous Polymerization Reactions. *Chem. Eng. Sci.* **1984**, *39*, 87–99. [CrossRef]
40. Pang, K.; Kotek, R.; Tonelli, A. Review of Conventional and Novel Polymerization Processes for Polyesters. *Prog. Polym. Sci.* **2006**, *31*, 1009–1037. [CrossRef]
41. Komorowska-Durka, M.; Dimitrakis, G.; Bogdał, D.; Stankiewicz, A.I.; Stefanidis, G.D. A Concise Review on Microwave-Assisted Polycondensation Reactions and Curing of Polycondensation Polymers with Focus on the Effect of Process Conditions. *Chem. Eng. J.* **2015**, *264*, 633–644. [CrossRef]
42. Gauthier, M.A.; Gibson, M.I.; Klok, H.-A. Synthesis of Functional Polymers by Post-Polymerization Modification. *Angew. Chem. Int. Ed.* **2009**, *48*, 48–58. [CrossRef] [PubMed]
43. Liu, Y.; Wang, W.; Wang, A. Effect of Dry Grinding on the Microstructure of Palygorskite and Adsorption Efficiency for Methylene Blue. *Powder Technol.* **2012**, *225*, 124–129. [CrossRef]
44. Kayabaşı, Y.; Erbaş, O. Methylene Blue and Its Importance in Medicine. *Demiroglu Sci. Univ. Florence Nightingale J. Med.* **2020**, *6*, 136–145. [CrossRef]
45. Khan, I.; Saeed, K.; Zekker, I.; Zhang, B.; Hendi, A.H.; Ahmad, A.; Ahmad, S.; Zada, N.; Ahmad, H.; Shah, L.A.; et al. Review on Methylene Blue: Its Properties, Uses, Toxicity and Photodegradation. *Water* **2022**, *14*, 242. [CrossRef]
46. Bharti, V.; Vikrant, K.; Goswami, M.; Tiwari, H.; Sonwani, R.K.; Lee, J.; Tsang, D.C.W.; Kim, K.-H.; Saeed, M.; Kumar, S.; et al. Biodegradation of Methylene Blue Dye in a Batch and Continuous Mode Using Biochar as Packing Media. *Environ. Res.* **2019**, *171*, 356–364. [CrossRef]
47. Electrochemical Degradation of Methylene Blue—ScienceDirect. Available online: https://www.sciencedirect.com/science/article/pii/S1383586606003455?casa_token=DYxwfvFVUQgAAAAA:vjMzUuZGPM6mpqqW_a0wQ90yQ05xxtJsA-4Q6EPyf6awcUdpqqdMpgLOIg9b6BvBvYfgfdUVGw (accessed on 17 September 2024).
48. Li, Q.; Li, Y.; Ma, X.; Du, Q.; Sui, K.; Wang, D.; Wang, C.; Li, H.; Xia, Y. Filtration and Adsorption Properties of Porous Calcium Alginate Membrane for Methylene Blue Removal from Water. *Chem. Eng. J.* **2017**, *316*, 623–630. [CrossRef]
49. Sivakumar, R.; Lee, N.Y. Adsorptive Removal of Organic Pollutant Methylene Blue Using Polysaccharide-Based Composite Hydrogels. *Chemosphere* **2022**, *286*, 131890. [CrossRef]
50. Zammuto, V.; Macrì, A.; Agostino, E.; Ruggeri, L.M.; Caccamo, M.T.; Magazù, S.; Campos, V.L.; Aguayo, P.; Guglielmino, S.; Gugliandolo, C. Enhancement of Biodegradation and Detoxification of Methylene Blue by Preformed Biofilm of Thermophilic Bacilli on Polypropylene Perforated Balls. *J. Mar. Sci. Eng.* **2024**, *12*, 1248. [CrossRef]
51. Rafatullah, M.; Sulaiman, O.; Hashim, R.; Ahmad, A. Adsorption of Methylene Blue on Low-Cost Adsorbents: A Review. *J. Hazard. Mater.* **2010**, *177*, 70–80. [CrossRef]
52. Wahyuni, E.T.; Alharrisa, E.Z.; Lestari, N.D.; Suherman, S. Modified Waste Polystyrene as a Novel Adsorbent for Removal of Methylene Blue from Aqueous Media. *Adv. Environ. Technol.* **2022**, *8*, 83–92. [CrossRef]
53. Kamani, M.; Rahmati, M.; Vandani, S.A.K.; Fard, G.C.; Kamani, M.; Rahmati, M.; Vandani, S.A.K.; Fard, G.C. Investigation of "MCM-22", "ZSM-12 & 35 COMPOSITE", and "ZEOLITE AL-MORDENITE & ZSM-39 COMPOSITE" crystals by analysis of characterization techniques. *J. Chil. Chem. Soc.* **2021**, *66*, 5332–5338. [CrossRef]